

FIFTH INTERNATIONAL CONGRESS ON SOUND AND VIBRATION

DECEMBER 15-18, 1997
ADELAIDE, SOUTH AUSTRALIA

Invited Paper

ACOUSTIC RADIATION FROM A TANDEM TWO-PLATE ARRAY IN A FLUID FLOW: DEPENDENCE ON ARRAY GEOMETRY AND FLOW REGIME

M.K. Bull, A.M. Blazewicz and J.M. Pickles

**Department of Mechanical Engineering, University of Adelaide,
South Australia, 5005, Australia.**

ABSTRACT

Acoustic radiation generated by fluid flow over an array of two plates of rectangular cross-section in tandem has a dominant, dipole, component of discrete frequency originating from force fluctuations on the downstream plate. The forces result from pressure fluctuations near the leading edge of the downstream plate, generated by interaction between the leading edge of the downstream plate and fluctuating flow in the gap between the plates. The intensity of acoustic radiation is strongly dependent on the flow regime which is established on the array.

The chord-to-thickness ratios C_1 and C_2 of the upstream and downstream plates define the array geometry. Two additional primary parameters determine the flow regime: (i) the ratio S of the length (or virtual length) of the separation bubble formed by the shear layers separating from the leading edges of the upstream plate to the plate thickness; and (ii) the ratio G of the gap between the plates to plate thickness. The value of S fluctuates with time between limits S_{min} and S_{max} . The flow regime established depends on the relative values of C_1 , C_2 , G , S_{min} and S_{max} . A classification of possible regimes is made on this basis.

Flow visualisations and experimental results are presented for arrays in which the leading plate has a square cross-section. It is shown that the flow regimes can be identified from discontinuities in the measured variation with G of pressures on the plates and the Strouhal numbers of periodic flow fluctuations within the gap. Corresponding discontinuities are found in the variation of intensity of acoustic radiation with G . The results clearly show that whenever the flow regime changes, the level of acoustic radiation changes correspondingly, and often dramatically.

1. INTRODUCTION

The results presented in this paper relate to a general study of flow over and acoustic radiation from two plates, of the same thickness and both of rectangular cross-section, in tandem. On such arrays, a large number of different flow regimes can be established. The plate geometry is defined by the chord lengths c_1 and c_2 of the upstream plate (*P1*) and downstream plate (*P2*) respectively, the plate thickness t , and the corresponding chord-to-thickness ratios $C_1 = c_1/t$ and $C_2 = c_2/t$. Once the plate geometry is specified, the flow regime, and consequently the acoustic radiation from the plates, is determined by just two additional parameters: the ratio $G = g/t$ of the streamwise gap g between the plates to the thickness; and the ratio $S = s/t$ of the length (or virtual length) s of the separation bubble formed by the shear layer separating from the leading edge of the upstream plate to the thickness.

The first of these, the gap parameter; determines the extent and nature of the interaction between shear layers separated from the leading edges of the upstream plate and the fluid in the gap. The flow in the gap may take the form of a periodic reversal of flow through the gap, a pair of stationary counter-rotating vortices within the gap, or a vortex street within the gap.

The second parameter S needs some explanation. In the context of a two-plate array, the notion of separation-bubble length is generalised to include not only the length of the bubble formed when a shear layer separated from one of the leading edges of the upstream plate does reattach somewhere on the array, but also the virtual length, the distance from the leading edge where the two separated shear layers from opposite leading edges merge or interact (either in the gap or downstream of the second plate) in the absence of reattachment. The length of the separation bubble fluctuates in time, between lower and upper limits, S_{min} and S_{max} . Their effective values depend on the geometry of any particular array, but will in general be similar to those for the leading-edge separation bubble on a long single plate, corresponding, typically, to $S \cong 5 \pm 2$ [1,2].

TABLE 1 Classification of flow regimes

Regime	C_1	$(C_1 + G)$	$(C_1 + G + C_2)$
A	$> S_{max}$		
B	$< S_{max}, > S_{min}$	$> S_{max}$	
C1		$< S_{max}$	$> S_{max}$
C2		$< S_{max}$	$< S_{max}$
D	$< S_{min}$	$> S_{max}$	
E1		$< S_{max}, > S_{min}$	$> S_{max}$
E2		$> S_{min}$	$< S_{max}$
F1		$< S_{min}$	$> S_{max}$
F2			$< S_{max}, > S_{min}$
F3			$< S_{min}$

The flow regimes can be classified (Table 1 and Figure 1), in a more general way than previously [3,4], according to the relative values of C_1 , C_2 , G , S_{min} and S_{max} . All of the regimes listed in Table 1 are not necessarily possible for every two-plate-array. There are two additional constraints. The first is the value of C_2 in relation to the overall excursion in S : if $C_2 < (S_{max} - S_{min})$, regime *F1* is not possible, while if $C_2 > (S_{max} - S_{min})$, regimes *C2*, *E2*, and *F3* cannot occur. The second is the value of $(C_1 + C_2)$ in relation to both S_{min} and S_{max} , which

may further restrict the number of possible regimes. The possible flow regimes can be usefully portrayed on a C_1 v. G diagram with C_2 as an additional parameter, in which case the detailed nature of the diagram depends on these two constraints.

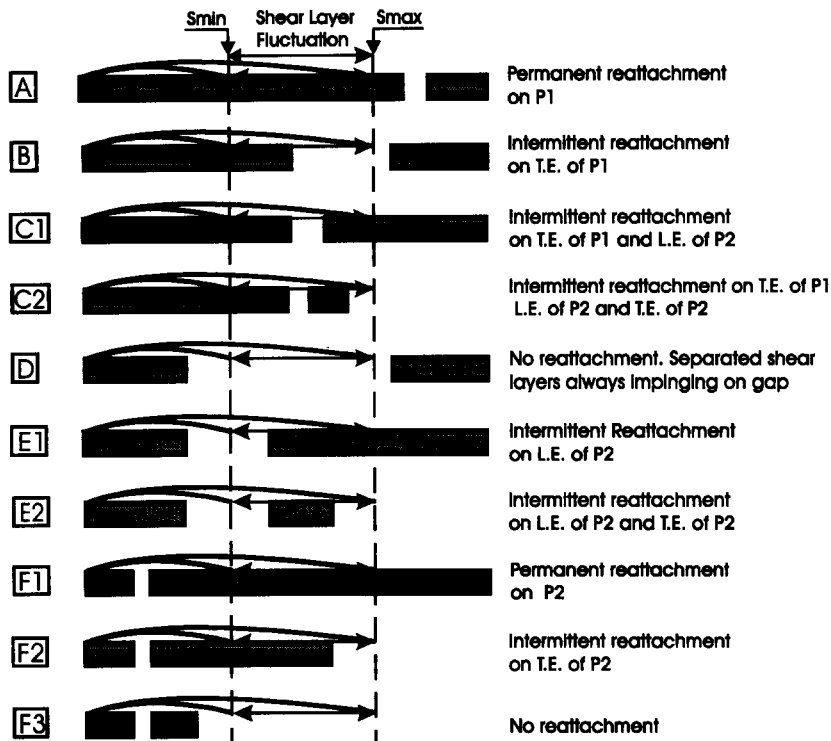


Figure 1. Schematic representation of possible flow regimes according to plate configuration in relation to separation bubble length.

To illustrate the effects of different combinations of the parameters, attention will be concentrated here on three tandem arrays:

(i) ($C_1 = 1, C_2 = 1$) array, consisting of two plates with square cross-section. Based on the single-plate data, we expect $C_1 < S_{min}$ and $C_2 < (S_{max} - S_{min})$. For values of C_2 satisfying the latter condition, the various possible flow regimes (anticipating values of S_{min} and S_{max} to be determined later) as a function of C_1 and G are shown in Figure 2(a). For $C_1 < S_{min}$, the possible flow regimes are D, E1, E2, F2 and F3.

(ii) ($C_1 = 1, C_2 = 6$) and ($C_1 = 1, C_2 = 9$) arrays, each consisting of a square upstream plate and a downstream plate of rectangular cross-section. For both, we expect $C_1 < S_{min}$ and $C_2 > (S_{max} - S_{min})$. The possible flow regimes (Figure 2(b)) are D, E1 and F1.

2. EXPERIMENTAL ARRANGEMENT

All of the measurements reported were carried out on plate arrays mounted between large end-plates and therefore in nominally two-dimensional flow. Flow visualisation was carried out in a water channel, using hydrogen bubbles as the visualisation medium, at flow speeds of up to 0.2 m/s. The plates had a span of 200 mm and thickness of 5.0 or 10.0 mm. Pressure and flow-fluctuation-frequency measurements (by surface pressure tappings and hot-wire anemometers respectively) were made in an open-jet wind-tunnel, at a speed of 13.0 m/s, on plates of span 690 mm and thickness 18 mm. Measurements (at the centres of faces) were made of base pressures on both plates in the arrays and of the pressure on the leading face of

the second plate. Acoustic measurements (sound pressure levels) were made on plates 4.0 mm thick in an air jet issuing into a large reverberant chamber, at a speed of approximately 65 m/s.

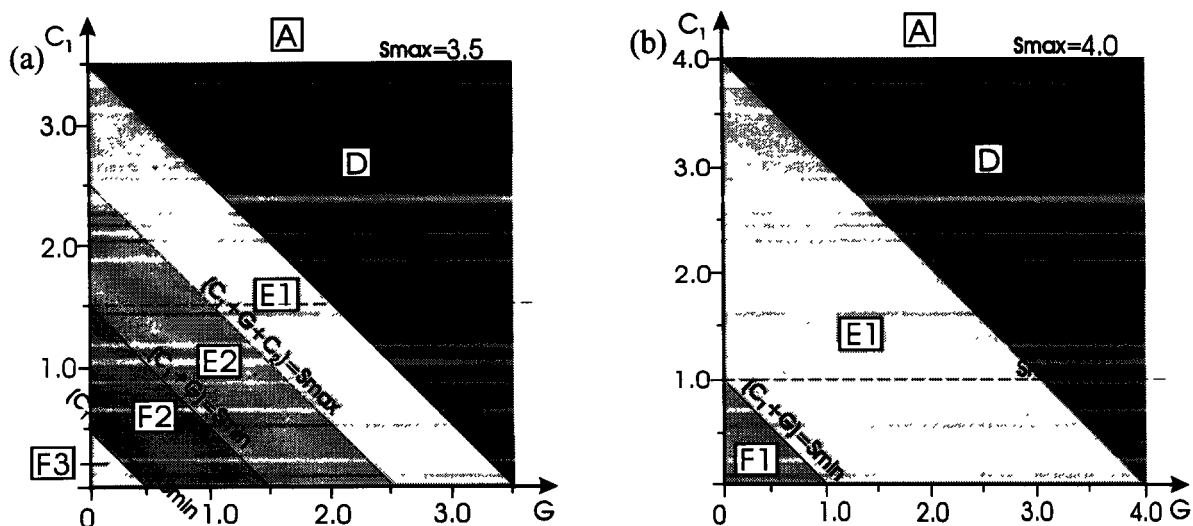


Figure 2. Flow regimes as a function of C_1 and G for (a) $C_2 < (S_{max} - S_{min})$ and (b) $C_2 > (S_{max} - S_{min})$.

3. RESULTS AND DISCUSSION

3.1 Flow visualisation

The flow regime which is established depends to some extent on the Reynolds number $Re_t = U_1 t / \nu$ (where U_1 is the free-stream velocity and ν the kinematic viscosity of the fluid) as well as on the array geometry. The effects of Reynolds number have been investigated by flow visualisation at $Re_t \cong 600, 1200$ and 1900 . These tests indicate that, as Reynolds number is increased, the size of gap characterising the onset of any particular flow regime decreases. This is equivalent to the effective values of S_{max} , S , and S_{min} decreasing with increasing Reynolds number. This behaviour is similar to that of leading-edge separation bubbles on single plates for $Re_t > 300$, as observed by Lane and Loehrke [1]. In the present work, wind-tunnel measurements of flow parameters and acoustic radiation have been made at much larger Reynolds numbers ($\sim 17,000$) than those achievable for flow visualisation. This leads to some uncertainties in associating measured surface pressures, flow-fluctuation frequencies and acoustic radiation levels with particular flow regimes.

3.1.1 The ($C_1 = 1, C_2 = 1$) array

In the present investigation, with $C_1 = 1$, the effects of Reynolds number are most noticeable at very small gaps. Flow visualisation shows that, at $Re_t \sim 600$, the regime $F3$ (which occurs on a single plate with $C = 2$) persists only for gaps up to $G \cong 0.2$. This regime, shown in Figure 3, is characterised by flow separation from the leading edges of plate $P1$, no reattachment, and vortex street formation downstream of plate $P2$. At $Re_t \sim 1900$, it could not be detected even at gap sizes as low as $G = 0.05$. It has therefore been concluded that this regime is not possible for the present array at higher Reynolds numbers. Hence, in the interpretation of the wind-tunnel and reverberation-chamber data for $Re_t \sim 17000$, it is assumed that the only possible regimes are $D, E1, E2$ and $F2$.

In regime $F2$, the shear layers separating from the leading edges of $P1$ reattach periodically and intermittently to the streamwise surfaces of $P2$, and form vortices downstream of $P2$. Reattachment alternates from one side of $P2$ to the other, and there is flow through the gap, the direction of which reverses periodically. Figure 4 shows a stage in the cycle when there is no reattachment on the upper surface of $P2$, flow in the gap is from top to bottom, and reattachment on the lower surface of $P2$ has just ceased.



Figure 3. ($C_1 = 1, C_2 = 1$) array. $G = 0.2$. $Re_t = 621$. Flow regime $F3$.



Figure 4. ($C_1 = 1, C_2 = 1$) array. $G = 0.5$. $Re_t = 621$. Flow regime $F2$.



Figure 5. ($C_1 = 1, C_2 = 1$) array. $G = 2$. $Re_t = 621$. Flow regime $E1$ with reattachment on $P2$.

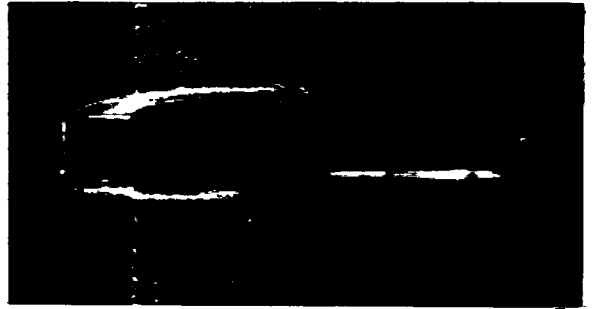


Figure 6. ($C_1 = 1, C_2 = 9$) array. $G = 0.5$. $Re_t = 621$. Flow regime $F1$

In regime $E2$, the separated shear layer intermittently rolls into the gap, intermittently reattaches to $P2$, or intermittently remains detached beyond $P2$; regime $E1$ is similar but only the first two of these processes occur. In practice, it is extremely difficult to distinguish between these two regimes on an array with $C_2 = 1$. An example of flow with reattachment on $P2$, is shown in Figures 5. The small vortices evident on the separated shear layers result from secondary (Kelvin-Helmholtz) instability of the vortex sheet; their frequency is very much higher than that of the main vortex street formed downstream of the array. When the gap becomes large, regime D is established, in which the separated shear layers penetrate the gap at all times and a vortex street is formed within the gap. For an array with $C_1 = 1$, this type of flow is very little influenced by the value of C_2 ; a typical example is shown in Figure 7.

3.1.2 The ($C_1 = 1, C_2 = 9$) array

At low Reynolds numbers and small gaps, typically $G \leq 1$, the flow regime is *F1* with reattachment on plate *P2* at all times (Figure 6). There is no flow through the gap, flow within the gap consists of a pair of trapped counter-rotating vortices, and the array behaves as a single plate. At larger gaps, $G > 1$, the flow regime becomes *E1*, with flow in the gap (including secondary vortex formation) very similar to that for the *E1* regime on the ($C_1 = 1, C_2 = 1$) array shown in Figure 5. At still larger gaps, $G > \sim 3$, regime *D*



Figure 7. ($C_1 = 1, C_2 = 9$) array. $G = 4$. $Re_t = 621$. Flow regime *D* with vortex street in gap

becomes established, with a vortex street within the gap (Figure 7). The regime *F1* appears not to persist to higher Reynolds numbers, and then only regimes *E1* and *D* occur.

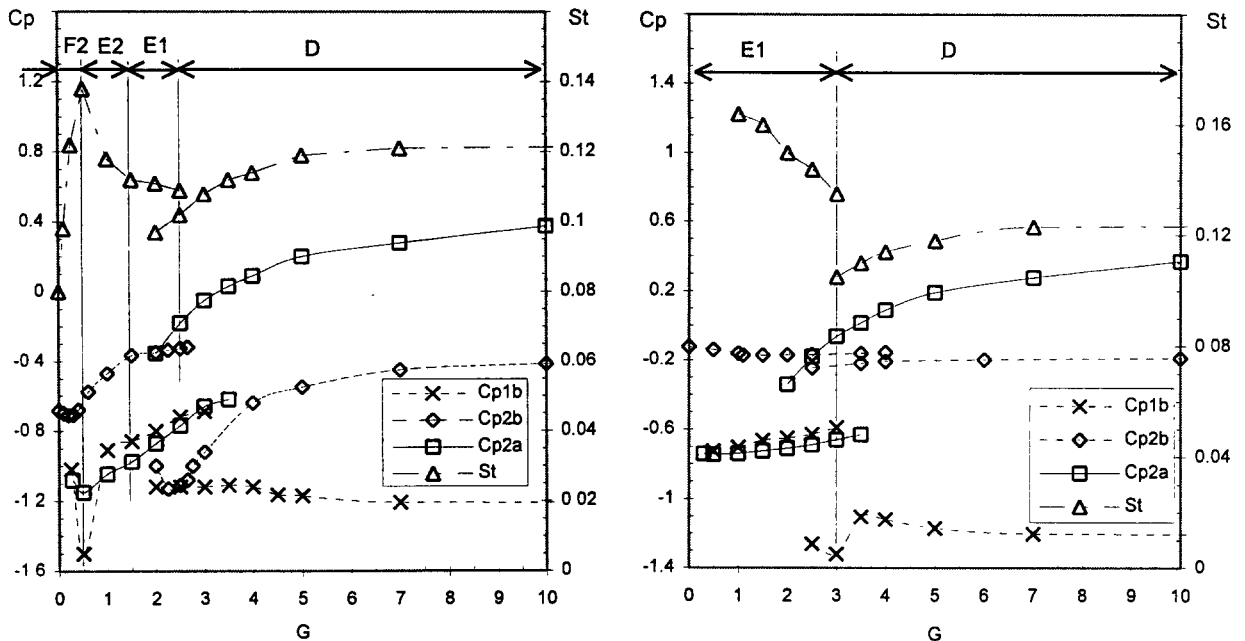


Figure 8. Dependence of Strouhal number and pressure coefficients on gap for (a) ($C_1 = 1, C_2 = 1$) array and (b) ($C_1 = 1, C_2 = 6$) array.

3.2 Vortex-shedding frequencies and surface pressures

Wind-tunnel data for pressure coefficients $C_p = (p - p_i)/1/2\rho U_i^2$ (where p is the surface pressure, p_i the free-stream static pressure and ρ the fluid density) and Strouhal numbers $St = ft/U_i$ (where f is flow-fluctuation or vortex-shedding frequency) for the ($C_1 = 1, C_2 = 1$) and ($C_1 = 1, C_2 = 6$) arrays are shown as a function of G in Figure 8. Pressure coefficients for the mid-points of the downstream face of *P1* (C_{p1b}), the upstream face of *P2* (C_{p2a}), and the downstream face of *P2* (C_{p2b}) are shown.

The Strouhal numbers shown are for frequencies measured in the gap. For the ($C_1 = 1, C_2 = 1$) array, at small gaps, this frequency is the same as that of the vortex street downstream of

the second plate; for the ($C_1 = 1, C_2 = 6$) array, vortex shedding takes place from the trailing edges of $P2$ at a frequency different from that of the flow fluctuations in the gap.

3.3 Flow regimes

From the considerations discussed in section 3.1, and from the different forms of variation of pressure coefficients and Strouhal numbers with gap size in different ranges of G which are evident in Figure 8, the ranges of G in which various flow regimes occur can be identified. In some cases there is an overlap range in which one or other of two regimes may occur. The ranges shown (and tabulated in Table 2) allow the effective values of the fluctuation limits of the separation bubble to be estimated. The values obtained are $S_{min} \cong 1.5$ and $S_{max} \cong 3.5$ for the ($C_1 = 1, C_2 = 1$) array and $S_{min} \cong 1.0$ and $S_{max} \cong 4.0$ for the ($C_1 = 1, C_2 = 6$) array.

Both arrays exhibit flow regimes $E1$ and D . Similarities in the variation of pressure and frequency parameters with G within these regimes clearly show that the extension of C_2 from 1 to 6 has very little effect on the flow over the upstream plate, the gap, and the leading edge of $P2$. This conclusion has implications for acoustic radiation due to flow over the arrays.

TABLE 2 High-Reynolds-number flow regimes.

$(C_1 = 1, C_2 = 1)$ ARRAY		
F2	$0 < G < [S_{min} - C_1]$	$0 < G < 0.5$
E2	$[S_{min} - C_1] < G < [S_{max} - (C_1 + C_2)]$	$0.5 < G < 1.5$
E1	$[S_{max} - (C_1 + C_2)] < G < [S_{max} - C_1]$	$1.5 < G < 2.5$
D	$G > [S_{max} - C_1]$	$G > 2.5$
$(C_1 = 1, C_2 = 6)$ ARRAY		
E1	$[S_{max} - (C_1 + C_2)] < G < [S_{max} - C_1]$	$0 < G < 3.0$
D	$G > [S_{max} - C_1]$	$G > 3.0$

3.4 Acoustic radiation

The variation of sound pressure level in the reverberation chamber with gap for $Re_t = 16,500$ is shown for both arrays in Figure 9. Although measurements have not been made for a large number of values of G , the general character of the dependence of acoustic radiation on gap can be established for both arrays, by using the conclusion reached in the preceding section. Previous investigations [3,5] have shown that the acoustic radiation is dipole in character, and dominated by a discrete component with the frequency of vortex or other periodically-fluctuating motion in the gap. It results from force fluctuations on the downstream plate, due predominantly to pressure fluctuations in the vicinity of the leading edges of the downstream plate, arising from the interaction between the edges and flow in the gap.

Because of the similarity of flow over the upstream plate and in the gap between the plates in the two arrays, the radiation from the arrays is also expected to be similar for the range of gaps over which flow regimes $E1$ and D occur. This similarity is evident for regime D . The dependence of the radiation on gap for regime $E1$ is established for the array with $C_2 = 6$; from it the gap dependence for the array with $C_2 = 1$ can be inferred, and is shown by a dashed line in Figure 9. For both arrays, a dramatic increase in acoustic radiation, by some 15 - 20 dB, occurs when the flow regime changes from $E1$ to D , i.e. when a regime of intermittent flow reattachment near the leading edges of $P2$ changes to one of an established vortex street in the gap.

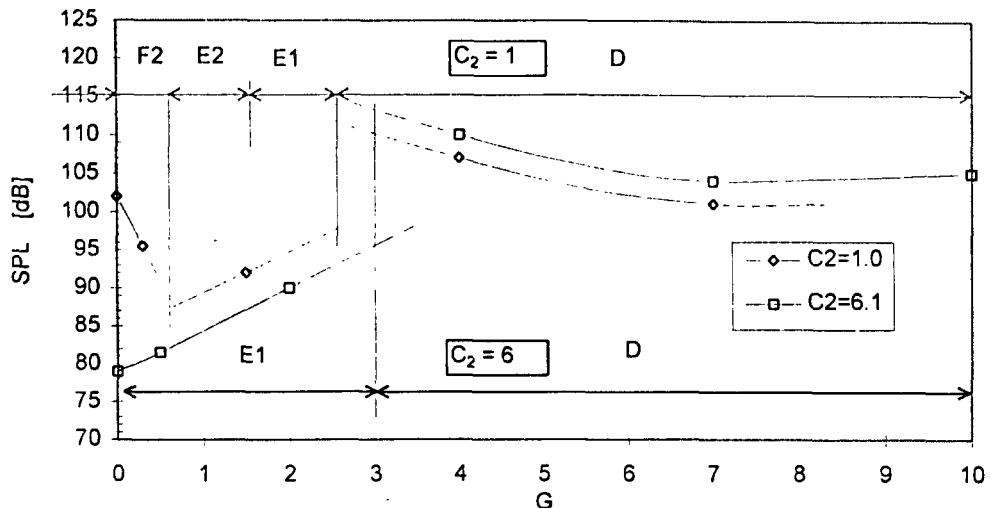


Figure 9. Acoustic radiation levels in reverberation chamber.

For the ($C_1 = 1$, $C_2 = 1$) array at small gaps, there is an additional dramatic change in the dependence of the radiation on G - from a rapid decrease to a rapid increase - when the flow regime changes from $F2$, one of intermittent reattachment only at the downstream end of $P2$, to $E2$, one involving intermittent reattachment to both upstream and downstream ends of $P2$.

4. CONCLUSION

A method of classification of possible regimes of flow over a tandem array of two plates of rectangular cross-section has been proposed, based on the premise that the regime is determined by the chord-to-thickness ratios of the two plates, the gap-to-thickness ratio, and the length-to-thickness ratio of the separation bubble formed by flow separation from the leading edges of the upstream plate. It has been shown that the different regimes can be identified by flow visualisation, and by different, characteristic, forms of variation of surface pressures and flow fluctuation frequencies with gap size.

The level of sound radiation from the array is strongly dependent on the flow regime established. This is well illustrated by arrays in which the leading plate is a square cylinder; in some cases, quite dramatic changes in the rate of change of radiation level with gap size or in the radiation level itself are found to accompany the change from one regime to another, particularly when transition to a regime with a vortex street in the gap occurs.

References

- [1] J.C. Lane, R.I. Loehrke J. Fluids Eng. **102**, 494, 1980.
- [2] M. Kiya, K. Sasaki, M. Arie. J. Fluid Mech., **219**, **120**, 1982.
- [3] A.M. Blazewicz, J.M. Pickles, M.K. Bull. Proc. Internoise 93, Leuven, 1631, 1993.
- [4] A.M. Blazewicz, M.K. Bull, J.M. Pickles Proc. 12th. Aust. Fl. Mech. Conf., 239, 1995.
- [5] M.K. Bull, J.M. Pickles, A.M. Blazewicz, D.A. Bies. Proc. Internoise 92, Toronto, 629, 1992